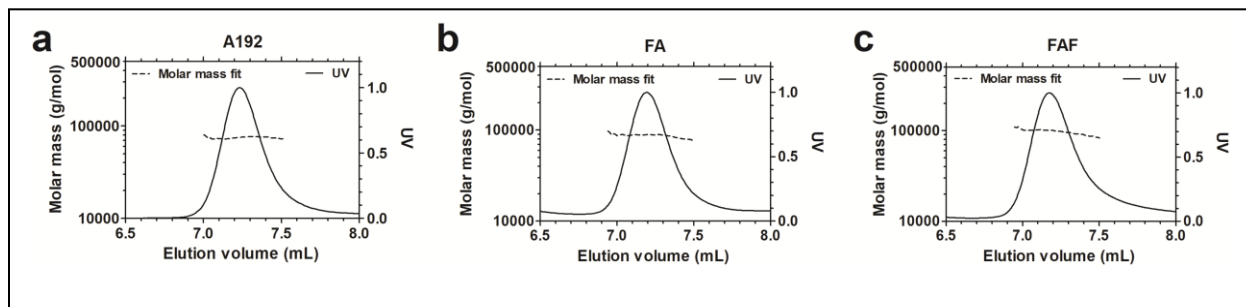
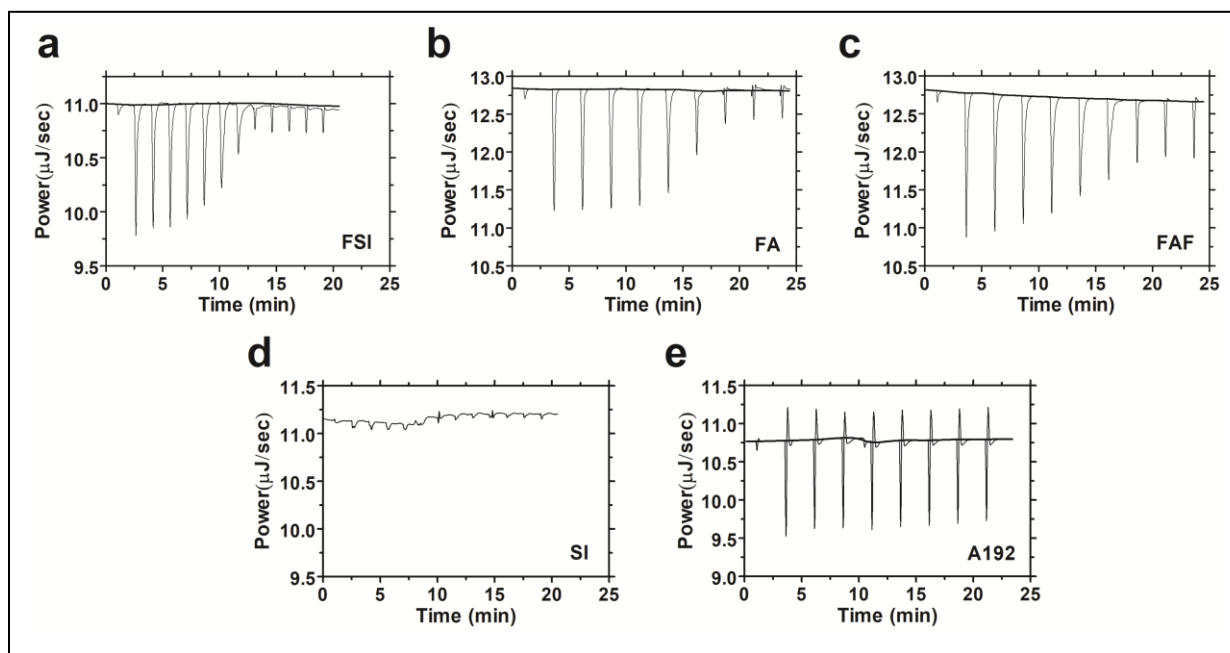


## Supplementary Data:



**Figure S1. A192, FA, and FAF display polypeptide morphology similar to hydrated polymeric coils.** In-line size exclusion chromatography coupled with multi-angle light scattering (SEC-MALS) analysis was performed on **(a)** A192; **(b)** FA; and **(c)** FAF in PBS at room temperature, which revealed an absolute molecular weight of 74.4 kDa, 85.7 kDa, and 96.8 kDa respectively; along with radii of gyration ( $R_g$ ) of  $11.9 \pm 0.9$  nm,  $16.4 \pm 1.6$  nm and  $13.8 \pm 0.4$  nm respectively. Using the  $R_h$  from DLS (**Table 1**),  $R_g/R_h$  was calculated as 1.72, 1.95 and 1.62 for A192, FA, and FAF respectively, which are characteristic ratios of hydrated coiled polymers.



**Figure S2. Saturable heat release during Rapa binding is observed only with FKBP-ELPs and not with backbone ELPs.** Raw binding isotherms generated using Isothermal Calorimetry by titrating Rapa against increasing concentrations of **(a)** FSI, **(b)** FA and **(c)** FAF shows decreasing power required to maintain zero temperature difference between calorimeter cell (containing Rapa) and reference cell (containing water) on successive injections of respective FKBP-ELPs into the calorimeter cell. Each power spike represents addition of respective FKBP-ELP into the calorimeter cell, which reaches saturation with time. With control ELPs **(d)** only heat of dilution for SI and **(e)** un-saturable heat of dilution for A192 was observed. Unlike for the FKBP-ELPs (FSI, FA, and FAF), the un-saturable raw isotherms (SI, A192) suggests no distinct binding between Rapa and control ELPs. A representative data set is shown from each group of  $n = 3$ .

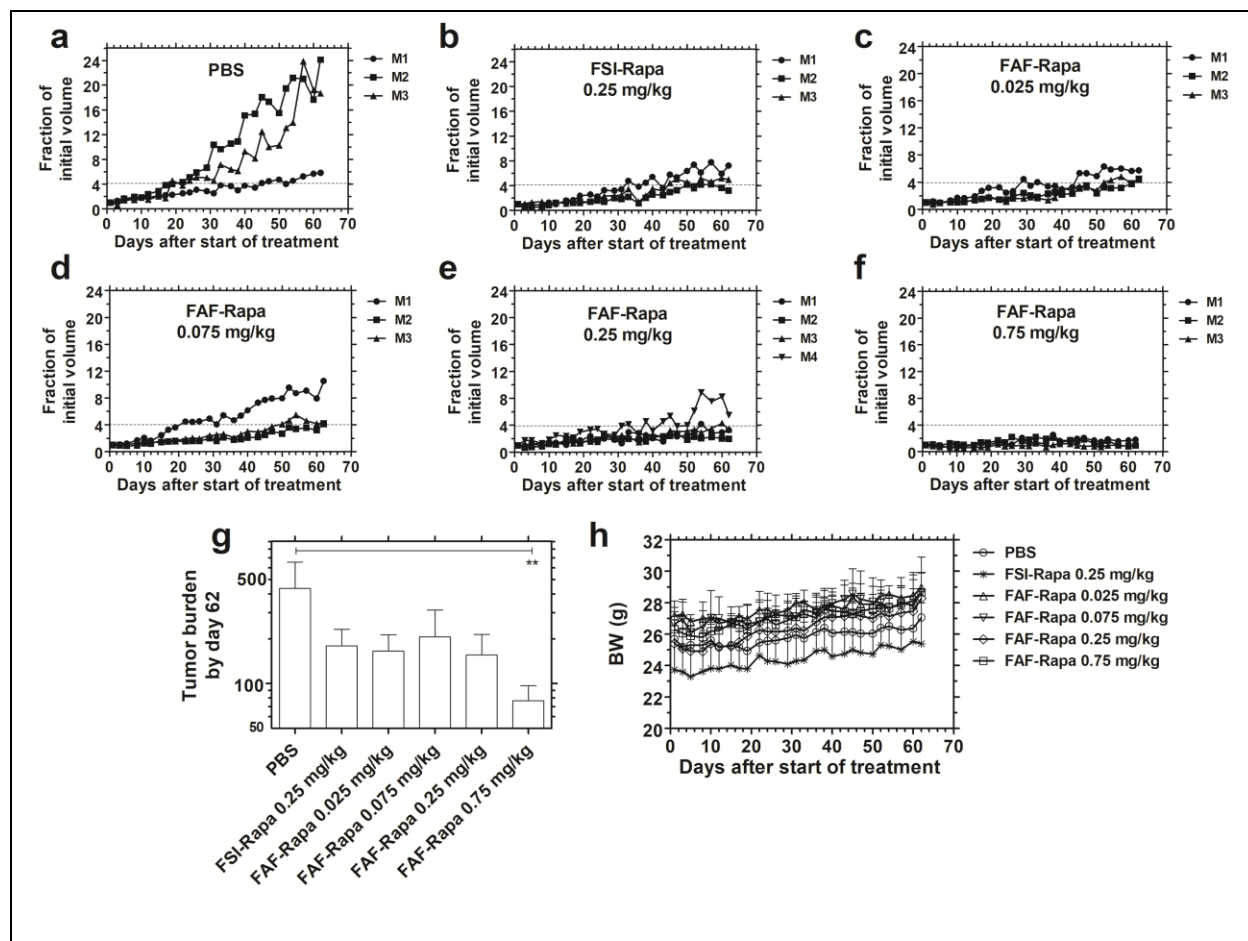


**Figure S3. FAF-Rapa demonstrates dose-dependent tumor growth suppression when injected IV.** Athymic nude mice ( $n=3-4$  per group) with orthotopic  $10-50 \text{ mm}^3$  MDA-MB-468 tumors were treated three times a week IV with **(a)** PBS, **(b)** FSI-Rapa at  $0.25 \text{ mg/kg}$ , **(c)** FAF-Rapa at  $0.025 \text{ mg/kg}$ , **(d)** FAF-Rapa at  $0.075 \text{ mg/kg}$ , **(e)** FAF-Rapa at  $0.25 \text{ mg/kg}$  and **(f)** FAF-Rapa at  $0.75 \text{ mg/kg}$ . **(g)** Tumor burden (Equation S4) by day 62 (mean  $\pm$  SD) was statistically significant for the comparison between PBS and FAF-Rapa at  $0.75 \text{ mg/kg}$  (Tukey's post-hoc analysis,  $\alpha = 0.05$ ,  $**p = 0.002$ ). **(h)** No decrease in body weight (mean  $\pm$  SD) over time was observed in any group, suggesting that the formulations were tolerated.

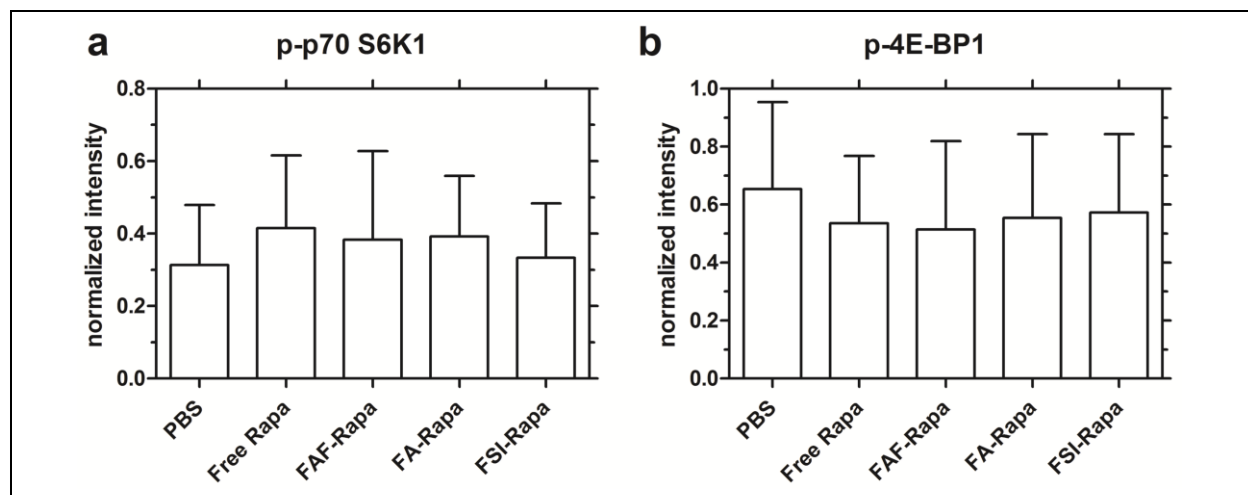


**Figure S4. SC treatment with Rapa at 0.75 mg/kg does not inhibit p-p70 S6K1 and p-4E-BP1 levels.** 1-way ANOVA on the normalized intensity levels (Equation S5) of **(a)** p-p70 S6K1 and **(b)** p-4E-BP1 ( $n = 4$ , mean  $\pm$  SD) showed no significant decrease between PBS and any treatment groups.

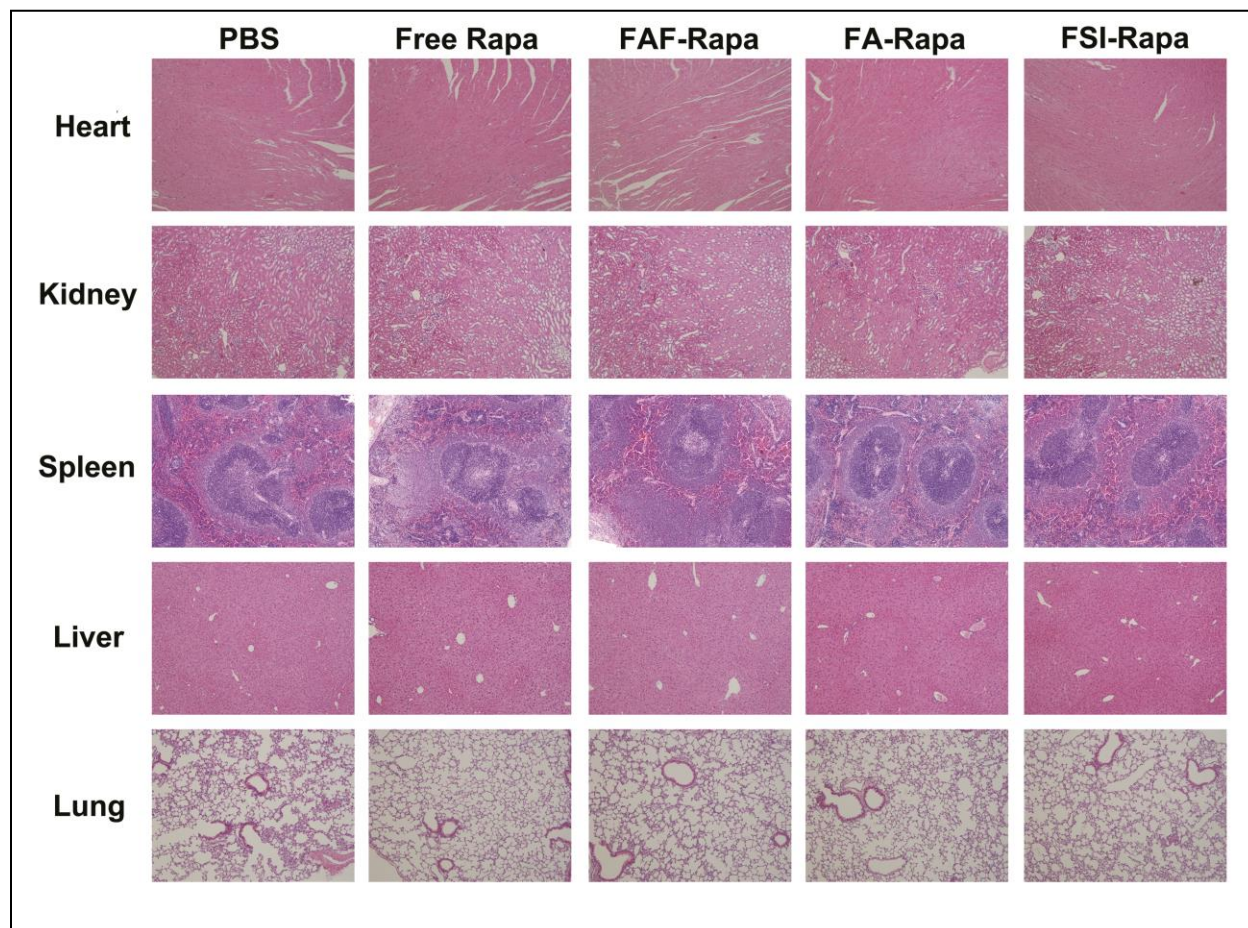


**Figure S5. Histopathology of mouse organs evaluated post SC treatment fails to show evidence of systemic toxicity across any treatment groups.** After the end of study, mice were perfused under anesthesia, euthanized and organs were evaluated for histopathology by H & E staining. No abnormal pathophysiology was reported in any of the organs evaluated across all the treatment groups. Organs from one representative mouse are shown from each group.

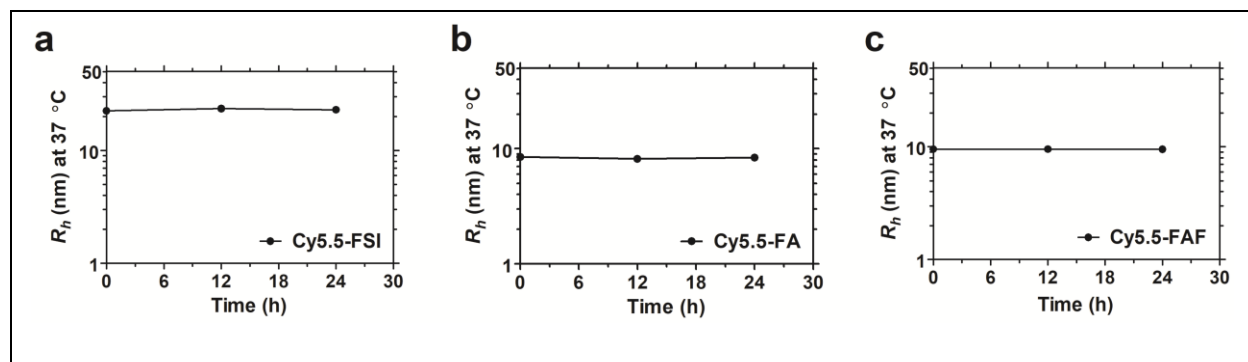


**Figure S6. Cy5.5 labeled FKBP-ELPs retained a stable hydrodynamic radius at 37 °C.** FKBP-ELPs post Cy5.5 labeling were characterized by dynamic light scattering before injecting *in vivo*. The  $R_h$  of **(a)** Cy5.5-FSI, **(b)** Cy5.5-FA and **(c)** Cy5.5-FAF remained stable for 24 h; furthermore, the particle size was consistent with that observed prior to Cy5.5 labeling (**Figure 2d, main manuscript**). Values are represented as mean  $\pm$  SD (n = 3).

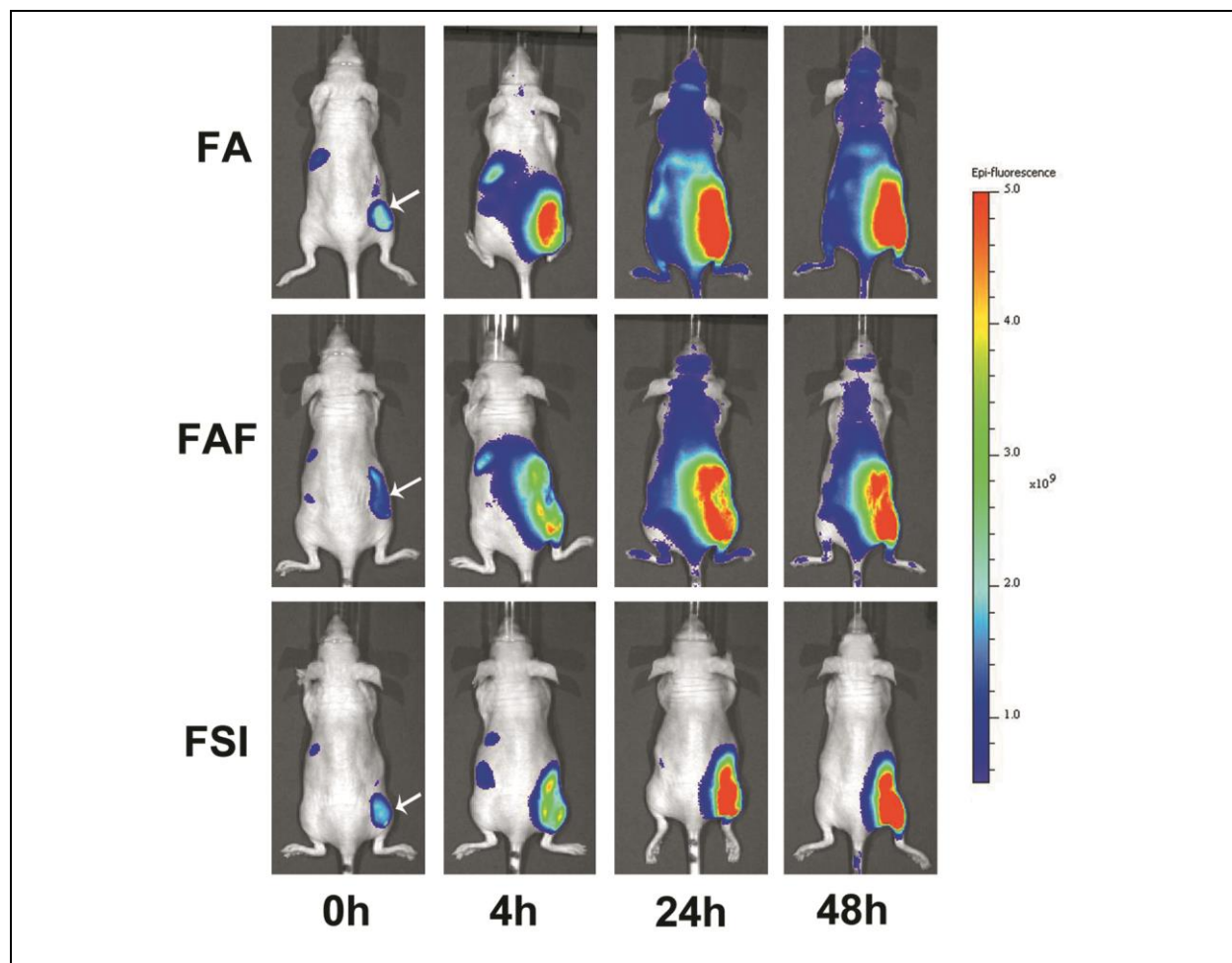


**Figure S7. Whole body scans of SC injected Cy5.5 labeled FKBP-ELPs taken dorsally.** FA, FAF and FSI show increased areas of fluorescence over time at site of SC injection. A single injection at the SC site at 0 h is shown as indicated by arrows. This high level of signal in the skin hindered tracking the bio-distribution of material in clearance organs, kidneys and liver for live mice; however, FA and FAF show greater whole body distribution compared to FSI. One representative mouse is shown from each group of  $n = 4$ .



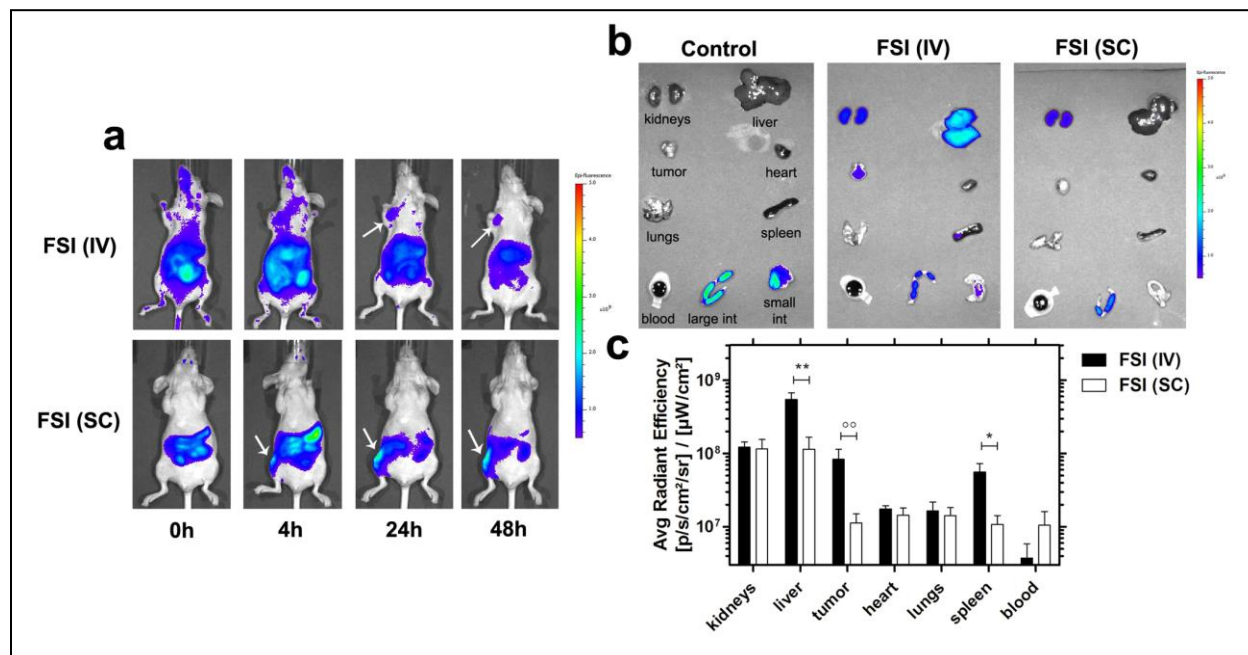


**Figure S8. Cy5.5-FSI injected IV shows greater whole body distribution and tumor accumulation compared to Cy5.5-FSI injected SC. (a)** MDA-MB-468 tumor implanted nude mice administered IV and SC with Cy5.5 labeled FSI were imaged using IVIS spectrum. FSI (IV) show high body-distribution and tumor accumulation compared to FSI (SC). Tumor accumulation and SC site of injection are shown as indicated by arrows. A representative mouse scan in ventral position at 0, 4, 24 and 48 h is shown from both the groups with  $n = 4$  mice. **(b)** After the 48 h whole body scan, mice were immediately euthanized and organs were scanned for fluorescence. A representative mouse is shown from each group of  $n = 4$ . **(c)** The fluorescence intensity in Avg. radiant efficiency ( $n = 4$ , mean  $\pm$  SD) was quantified by drawing ROIs on all the organs. Paired t-test analysis revealed statistical significance between FSI (IV) and FSI (SC) in liver, tumor and spleen respectively ( $\alpha = 0.05$ , \*\* $p = 0.001$ ,  $^{\circ\circ}p = 0.008$ , \* $p = 0.01$ ).



## Supplemental Methods:

### FKBP-ELP physicochemical characterization.

To determine ELP purity, 6-12  $\mu\text{g}$  protein was mixed with SDS Laemmli loading buffer (1610747, Bio-Rad, Hercules, CA) containing 10% v/v  $\beta$ -mercaptoethanol, heated at 90°C for 5 mins and loaded onto 4-20% gradient Tris-Glycine-SDS PAGE gel (58505, Lonza, Walkersville, MD) for electrophoresis. The gel was stained using 10% w/v copper chloride and imaged using a ChemiDoc™ Touch Imaging system (Bio-Rad) (**Figure 2a**). Picture was imported into ImageJ (National Institutes of Health, Bethesda, MD), individual lanes were selected and an intensity profile was extracted. The peak areas per gel lane were calculated and purity was estimated using the following equation:

$$\% \text{ purity} = \frac{A_{peak}}{A_{tot}} \times 100 \quad \text{Equation S1}$$

where  $A_{peak}$  is the area of the protein band peak and  $A_{tot}$  is the total area under all the peaks per lane.

Observed molecular weights of all the constructs were determined by mixing 25  $\mu\text{M}$  protein samples with 10 mg/mL sinapinic acid in 50% ACN, 0.1% TFA, air dried, and analyzed on Microflex-TOF/TOF mass spectrometer (Bruker Daltonics, Billerica, MA) in positive ion, linear mode (**Table 1**). Temperature-concentration phase diagrams were obtained by measuring optical density at 350 nm on a UV-Vis DU 800 spectrophotometer (Beckman Coulter, Brea, CA). A temperature ramp (1 °C/min, measured every 0.3 °C) was performed for different concentrations of FKBP-ELPs with and without Rapa loading using thermal mount microcells (Beckman Coulter). Phase transition temperatures were defined where the first derivative of the optical density vs. temperature was maximal (**Figure 2 b, c**). The data points were fit with the following linear relationship:

$$T_t = b - m [\text{Log}_{10}(\text{concentration})] \quad \text{Equation S2}$$

where  $b$  is the intercept temperature (°C) at a reference concentration of 1  $\mu\text{M}$  and  $m$  is the slope, which can be interpreted as the decrease in  $T_t$  upon a 10-fold increase in concentration.

Particle sizes and stability were evaluated by measuring the hydrodynamic radius ( $R_h$ ) using DLS (**Figure 2 d, e**). 25  $\mu$ M concentration samples were filtered through 200 nm sterile Acrodisc® 13 mm filters (PN 4454, Pall Corporation). 60  $\mu$ L of each sample was loaded in triplicate in a 384 well black plate (781096, Greiner Bio One, Monroe, NC) and covered with 20  $\mu$ L mineral oil. The plate was gently centrifuged at 15 °C to remove air bubbles and  $R_h$  was measured using the Wyatt Dynapro plate reader (Santa Barbara, CA) from 20-37 °C at intervals of 1 °C (**Figure 2d**). The stability of Rapa loaded FKBP-ELPs was evaluated at 37 °C for 48 h to study the effect of drug binding on the size and structural properties of FKBP-ELPs (**Figure 2e**). The reported values are presented as mean  $\pm$  SD (n=3). The polypeptide conformation of A192, FA and FAF was interpreted and analyzed at room temperature using SEC-MALS. 100  $\mu$ g protein was injected into a shodex KW-803 size exclusion column using sterile filtered PBS at the rate of 0.5 ml/min and eluents were analyzed on a Wyatt Helios light scattering detector (Santa Barbara, CA). Data was fit to a Debye plot to determine the  $R_g$  and absolute molecular weight. The  $R_g/R_h$  ratio was used to interpret polypeptide morphology (**Figure S1**).

#### **Drug loading and formulation preparation for *in vivo* administration.**

Drug loading was performed using two-phase solvent evaporation technique. 200-400  $\mu$ M FKBP-ELP (2 mL) in PBS was equilibrated in a glass vial at 35 °C for 10 mins followed by addition of 200-400  $\mu$ M Rapa (2mL for FSI loading and 6 mL for FA/FAF loading) in a hexane/EtOH mixture (70/30 % v/v) to obtain a two-phase mixture of FKBP-ELP in PBS at the bottom and Rapa in hexane at the top. The organic phase was evaporated under mild flow of dry N<sub>2</sub> gas with continuous stirring on a magnetic stir plate over 10-15 mins and the remaining aqueous solution containing Rapa loaded FKBP-ELPs was centrifuged (13000 RPM, 10 min, 37 °C) to remove free drug pellet. Centrifugation of the supernatant was repeated until no precipitate was observed. FSI-Rapa was dialyzed overnight in PBS at 4 °C to remove the fast-eluting drug from the hydrophobic core, as observed previously [1]. The supernatant was filtered using 200 nm sterile Acrodisc® 25 mm filters

(PN 4612, Pall Corporation) and Rapa concentration was determined at 280 nm by C-18 RP-HPLC column (186003033, Waters, Milford, MA) using a calibrated Rapa standard curve. The RP-HPLC run was performed using mobile phase A (water with 0.1% TFA) and phase B (methanol with 0.1% TFA) using a gradient from 40% to 95% of phase B. Post quantification, drug-loaded formulations were diluted in Dulbecco's sterile PBS buffer (PBL01, Caisson labs, Smithfield, UT) to concentrations required for the indicated dosage (mg/kg BW) and frozen at -80 °C as aliquots for single use.

### **Tumor regression studies.**

A single injection of 1-2 x 10<sup>6</sup> MDA-MB-468 cells in 100 µL FBS free media supplemented with 4 mg/mL matrigel (354262, Corning®) was implanted into the right mammary fat pad of 7-8 weeks old female athymic nude mice (Nude-*Foxn1<sup>nu</sup>*, Envigo Inc, Indianapolis, IN). Mice were randomized into groups and IV treatment was started with a tumor size of 10-50 mm<sup>3</sup>. Tumor implanted mice were treated with 100 µL injections of PBS, FSI-Rapa (0.25 mg/kg) and dose escalation of FAF-Rapa (0.025 - 0.75 mg/kg), which amounts to 70 µM FSI and 3 - 100 µM FAF in final injections. (**Figure S3**). Mice displaying ulcerated tumors were removed from the study. Tumor size and BW was measured thrice a week and tumor volume was calculated using the following equation:

$$\text{Tumor Volume (mm}^3\text{)} = \frac{a^2 \times b \times \pi}{6} \quad \text{Equation S3}$$

where *a* and *b* represents smaller and bigger tumor length respectively, measured with an electronic caliper. To capture variability in tumor-take, individual tumors were tracked over the duration of the study as fraction of their initial volume on day 1. For statistical comparison, the tumor burden by the last day of treatment was compared between treatment groups. Tumor burden was defined by the area under the growth curve in each mouse using the trapezoidal method as follows:

$$\text{Tumor Burden} = \sum_{i=1}^{t_{last}} \left[ \frac{(f_{i+1} + f_i)(t_{i+1} - t_i)}{2} \right] \quad \text{Equation S4}$$

where  $f_i$  is fraction of initial tumor volume observed on day  $t_i$ . To ensure homogeneity of variance, the  $\log_{10}$  transformed tumor burden (Eq. S4) by the last day of treatment was compared with 1-way ANOVA between all the 6 groups ( $\alpha = 0.05$  with 95% CI,  $p = 0.006$ ). Tukey-Kramer post-hoc analysis was performed to test significance between the individual groups as reported in the results (**Figure S3 g**). Body weights are shown as mean  $\pm$  SD (**Figure S3 h**).

#### **Tumor western blot analysis.**

80  $\mu$ g total protein was mixed with SDS Laemmli loading buffer containing 10% v/v  $\beta$ -mercaptoethanol, heated at 90°C for 5 mins and loaded onto SDS-PAGE gels for electrophoresis. Separated protein bands were transferred onto a nitrocellulose membrane (IB23002, Thermo Fischer Scientific). Membrane was blocked for 1 hour at room temperature with 5% w/v nonfat dry milk in tris buffered saline (TBS) supplemented with 0.1% v/v Tween 20 (TBST - 200 mM Tris, 1.5 M NaCl, pH 7.6) followed by immunoblotting with primary monoclonal antibodies for p-p70 S6K1, p-4E-BP1, p-rpS6 and GAPDH (9234P, 13443S, 4858S, 5174 respectively, Cell Signaling Technology, Danvers, MA). All antibodies were diluted in TBST supplemented with 5% w/v Bovine Serum Albumin (A9647, Sigma-Aldrich). After immunoblotting the membrane overnight at 4 °C with gentle shaking, the membrane was washed with TBST (3x, 10 min) and incubated with secondary horseradish peroxidase (HRP)-linked antibody (7074, Cell signaling Technology) for 90 min at room temperature. The membrane was then washed with TBST (3x, 10 min) and incubated with HRP substrate (E2400, Denville Scientific, Holliston, MA) for 1 min prior to imaging using chemiluminescence (ChemiDoc™ Touch Imaging system, Bio-Rad). The membrane was stripped of primary antibodies using stripping buffer (46430, Thermo Fischer Scientific) for 45 min at room temperature and immunoblotted for GAPDH, which was used as an internal loading control. Protein expression levels were quantified using Image J analysis (**Figure 7a**) on 8-bit, inverted images using the following equation:

$$\text{Normalized intensity} = \frac{I_{\text{protein}}}{I_{\text{GAPDH}}} \quad \text{Equation S5}$$

where  $I_{protein}$  is the integrated density of p-p70 S6K1, p-4E-BP1 or p-rpS6 band and  $I_{GAPDH}$  is the integrated density of respective GAPDH band.

### Cy5.5 labeling of FKBP-ELPs.

FA, FAF, and FSI in PBS were mixed with three molar excess of Cy5.5 NHS ester (47020, Lumiprobe, Hallandale Beach, Florida) solubilized in DMSO and incubated overnight at 4 °C. Excess unreacted Cy5.5 was removed by loading the reaction mixture twice onto PD-10 desalting columns (17-0851-01, GE Healthcare Life Sciences). Labeled fractions were identified using SDS-PAGE and concentrated ten-fold using spin concentrators (UFC503024, Amicon Ultra, 30 kDa MWCO). The labeled material was quantified with a labeling efficiency of ~15 % on a UV-Vis spectrophotometer using the following equations:

$$C_{Cy5.5} = \frac{A_{679} \times dilution\ factor}{209000 \times l} \quad \text{Equation S6}$$

$$C_{FKBP-ELP} = \frac{[A_{280} - (0.09 \times A_{679})] \times dilution\ factor}{MEC_{FKBP-ELP} \times l} \quad \text{Equation S7}$$

$$\text{Labeling efficiency (\%)} = \frac{C_{Cy5.5}}{C_{FKBP-ELP}} \times 100 \quad \text{Equation S8}$$

### Supplementary references.

1. Shi P, Aluri S, Lin YA, Shah M, Edman M, Dhandhukia J, et al. Elastin-based protein polymer nanoparticles carrying drug at both corona and core suppress tumor growth in vivo. *J Control Release*. 2013; 171: 330-8.